The Astrophysical Journal, 701:1665–1672, 2009 August 20 doi:10.1088/0004-637X/701/2/1665

SUBARU HIGH-RESOLUTION SPECTROSCOPY OF STAR G IN THE TYCHO SUPERNOVA REMNANT*

Wolfgang E. Kerzendorf[1], Brian P. Schmidt[1], M. Asplund[2], Ken'ichi Nomoto[3,7], Ph. Podsiadlowski[4], Anna Frebel[5], Robert A. Fesen[6], and David Yong[1]

[1] Research School of Astronomy and Astrophysics, Mount Stromlo Observatory, Cotter Road, Weston Creek, ACT 2611, Australia; wkerzend@mso.anu.edu.au, brian@mso.anu.edu.au, yong@mso.anu.edu.au

[2] Max-Planck-Institut für Astrophysik, Karl-Schwarzschild-Straße 1, Postfach 1317, D-85748 Garching, Germany

[3] Institute for the Physics and Mathematics of the Universe, University of Tokyo, 5-1-5 Kashiwanoha, Kashiwa, Chiba 277-8568, Japan; nomoto@astron.s.u-tokyo.ac.jp

[4] Department of Astrophysics, University of Oxford, Oxford, OX1 3RH, UK; podsi@astro.ox.ac.uk

[5] McDonald Observatory, The University of Texas, 1 University Station C1402, Austin, TX 78712-0259, USA; anna@astro.as.utexas.edu

[6] Department of Physics and Astronomy, 6127 Wilder Laboratory, Dartmouth College, Hanover, NH 03755, USA; fesen@snr.dartmouth.edu

Received 2008 May 20; accepted 2009 May 27; published 2009 August 4

ABSTRACT

It is widely believed that Type Ia supernovae (SNe Ia) originate in binary systems where a white dwarf accretes material from a companion star until its mass approaches the Chandrasekhar mass and carbon is ignited in the white dwarf's core. This scenario predicts that the donor star should survive the supernova (SNe) explosion, providing an opportunity to understand the progenitors of SNe Ia. In this paper, we argue that rotation is a generic signature expected of most nongiant donor stars that is easily measurable. Ruiz-Lapuente et al. examined stars in the center of the remnant of SN 1572 (Tycho SN) and showed evidence that a subgiant star (Star G by their naming convention) near the remnant's center was the system's donor star. We present high-resolution ($R \simeq 40{,}000$) spectra taken with the High Dispersion Spectrograph on Subaru of this candidate donor star and measure the star's radial velocity as 79 ± 2 km s^{-1} with respect to the local standard of rest and put an upper limit on the star's rotation of 7.5 km s^{-1}. In addition, by comparing images that were taken in 1970 and 2004, we measure the proper motion of Star G to be $\mu_l = -1.6 \pm 2.1$ mas yr^{-1} and $\mu_b = -2.7 \pm 1.6$ mas yr^{-1}. We demonstrate that all of the measured properties of Star G presented in this paper are consistent with those of a star in the direction of Tycho SN that is not associated with the SN event. However, we discuss an unlikely, but still viable scenario for Star G to be the donor star, and suggest further observations that might be able to confirm or refute it.

Key words: astrometry – binaries: close – supernova remnants – supernovae: general – techniques: spectroscopic

Online-only material: color figure

1. INTRODUCTION

Type Ia supernovae (SNe Ia) are of broad interest. They serve as physically interesting endpoints of stellar evolution, are major contributors to galactic chemical evolution, and serve as one of astronomy's most powerful cosmological tools.

It is therefore unfortunate that the identity of the progenitors of SNe Ia is still uncertain. For example, without knowing the progenitors, the timescales of SNe Ia enriching the interstellar medium (ISM) with iron remains highly uncertain. But it is the crippling impact on the cosmological application of these objects which is especially profound; it is impossible to predict the consequences of any cosmological evolution of these objects or even gauge the likelihood of such evolution occurring.

There is broad agreement that the stars which explode as SNe Ia are white dwarfs which have accreted material in a binary system until they are near the Chandrasekhar mass, then start to ignite carbon explosively, which leads to a thermonuclear detonation/deflagration of the star. It is the identity of the binary companion that is currently completely undetermined. Suggestions fall into two general categories (Iben 1997):

1. Single-degenerate systems in which a white dwarf accretes mass from a nondegenerate companion, where the companion could be a main-sequence star, a subgiant, a red giant, or possibly even a subdwarf.
2. Double-degenerate systems where two CO white dwarfs merge, resulting in a single object with a mass above the Chandrasekhar limit.

The detection of circumstellar material around SN 2006X (Patat et al. 2007) has provided support for the single-degenerate model in this case, although the lack of substantial hydrogen in several other SNe Ia (Leonard 2007) poses more of a challenge to this scenario.

These models also make different predictions for the nature of the system following the explosion. In the double-degenerate case, no stellar object remains, but for a single white dwarf, the binary companion remains largely intact.

In the single-degenerate case, the expected effect of the supernova (SN) on the donor star has been investigated by Marietta et al. (2000), who have calculated the impact of an SN Ia explosion on a variety of binary companions. Canal et al. (2001) have explored many of the observational consequences of the possible scenarios, and Podsiadlowski (2003) has presented models that follow both the presupernova accretion phase and the postexplosion nonequilibrium evolution of the companion star that has been strongly perturbed by the impact of the SN shell. To summarize these results, main-sequence and subgiant companions lose 10%–20% of their envelopes and have a resulting space velocity of 180–320 km s^{-1}. Red giant companions lose most of its hydrogen envelope, leaving a helium core with a small amount of hydrogen-rich envelope

* Based in part on data collected at Subaru telescope, which is operated by the National Astronomical Observatory of Japan.

[7] Also at Department of Astronomy & Research Center for the Early Universe, School of Science, University of Tokyo, Bunkyo-ku, Tokyo 113-0033, Japan.

material behind, and acquire a space velocity of about 10–100 km s^{-1}. Pakmor et al. (2008) have used a binary stellar evolution code on a main-sequence star and exposed the evolved star to an SN Ia. Their simulations show that even less material is stripped due to the compact nature of a star that evolved in a binary. We will use their results where applicable.

Ruiz-Lapuente et al. (2004, henceforth RP04) have identified what might be the donor star to Tycho SN, an SN Ia which exploded in the Milky Way in 1572. These authors presented evidence that this star, Star G by their naming convention, is at a distance consistent with the Tycho supernova remnant (henceforth SNR), has a significant peculiar radial velocity and proper motion, roughly solar abundance, and a surface gravity lower than a main-sequence star. However, Star G is located at a significant distance from the inferred center of the remnant, and any process that has displaced the star must preserve the remnant's nearly perfectly circular projected shape. During the final stages of refereeing of this paper, we were made aware of the paper by Hernandez et al. (2009, henceforth GH09), who used Keck HIRES data to better constrain Star G's stellar parameters, and in addition, found an enhancement in nickel abundance, relative to normal metal-rich stars.

Ihara et al. (2007) have looked for Fe absorption lines from the remnant, using nearby stars as continuum sources, with the hope to better constrain the distance of these stars to the SNR. With their technique, stars in the remnant's center should show strong blueshifted Fe absorption lines, formed by material in the expanding shell of Fe-rich material from the SN, moving toward the observer. Stars in the foreground would show no Fe absorption, and background stars both red- and blueshifted absorption. Their study shows that Star G does not contain any significant blueshifted Fe absorption lines, suggesting that Star G is in the remnant's foreground. However, these observations and their analysis, while suggestive, cannot be considered as a conclusive rebuttal of Star G's association with the remnant; this technique requires a significant column depth of Fe which is not guaranteed. A lack of Fe column depth may be indicated by the fact that no stars were found in the vicinity of the remnant that showed both blue- and redshifted absorption lines.

To further examine the RP04 suggested association of Star G with the SN Ia progenitor, we have obtained a high-resolution spectrum of the star using Subaru and its High Dispersion Spectrograph (HDS; Noguchi et al. 1998).

We summarize, in Section 2, the observational circumstances of the Tycho remnant and any donor star, and argue in Section 3 that rapid rotation is an important, previously unrealized signature in an SN Ia donor star. In Section 4, we describe our Subaru observations. Section 5 covers the analysis of data and the results of this analysis. Section 6 compares the relative merit for Star G being the donor star to the Tycho SN or being an unrelated background star, and in Section 7 we summarize our findings and motivate future observations.

2. OBSERVATIONAL CHARACTERISTICS OF THE TYCHO REMNANT AND STAR G

RP04 have done a thorough job summarizing the relevant details of the Tycho remnant. The remnant shows the characteristics expected of an SN Ia based on its light curve (measured by Tycho Brahe himself), chemical abundances, and current X-ray and radio emission (Ruiz-Lapuente 2004). In Figure 1, we have overlaid radio contours on an optical image and have marked the position of the stars mentioned in this and RP04's work.

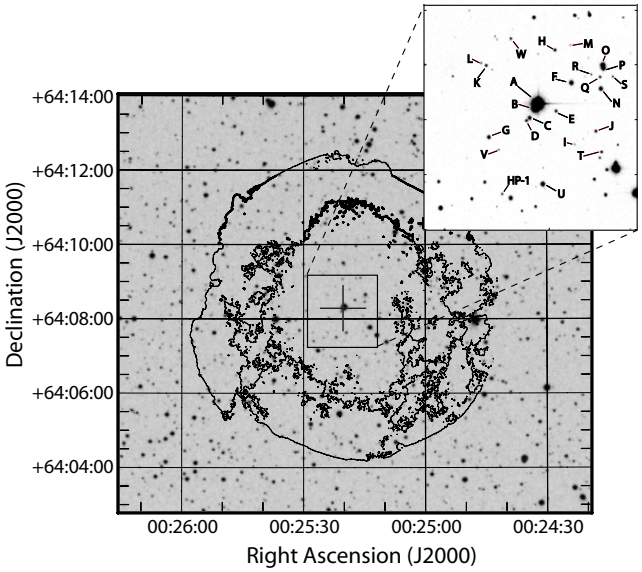

Figure 1. Radio contours (VLA Data Archive Project AM0347) have been overlaid (Gooch 1996) on an *R*-band image (NGS-POSS). The cutout is an INT image (see Section 5.3). The stars marked in the figure are mentioned in this work and in RP04's work.

Although it is not easy to measure the remnant's distance precisely, RP04 estimated Tycho's SNR distance to be 2.8 ± 0.8 kpc, using the ratio of the SN 1006 and Tycho SNR's angular sizes and their relative ages, and the direct distance measure of SN 1006 by Winkler et al. (2003). Krause et al. (2008) have recently shown, from a spectrum of a light echo associated with the SN 1572, that this SN was a normal SN Ia. Using Tycho's observed light curve, the properties of SN Ia as standard candles, and an extinction value, they find a distance to the SN of $3.8^{+1.5}_{-1.1}$ kpc. Updating their values for the extinction values determined in this paper (Section 6.1), as well as using an absolute magnitude for SN Ia of -19.5 ± 0.25 (Altavilla et al. 2004), we find a distance of $3.4^{+1.3}_{-1.0}$ kpc. In summary, we believe the remnant's distance is poorly constrained, but probably between 2 and 4.5 kpc. RP04 also report the spectroscopic and photometric properties for the bright stars near the center of the Tycho remnant and find a uniform value of approximately $E(B-V) = 0.6$ for stars more distant than 2 kpc. GH09 have revised the $E(B-V)$ value for Star G to 0.76.

In addition, for a select list of stars, RP04 provide radial velocities and proper motions. For Star G, RP04 report a value of $v_r = -99 \pm 6$ km s^{-1} for the radial velocity in the local standard of rest (henceforth LSR), a proper motion of $\mu_b = -6.1 \pm 1.3$ mas yr^{-1}, $\mu_l = -2.6 \pm 1.3$ mas yr^{-1}, $\log g = 3.5 \pm 0.5$, and $T = 5750$ K. Using HIRES data GH09 have improved the measurements of Star G's stellar parameters, finding $v_r \approx -80$ km s^{-1}, $\log g = 3.85 \pm 0.3$, $T = 5900 \pm 100$ K, and [Fe/H] $= -0.05 \pm 0.09$ dex. We note that Ihara et al. (2007) have classified Star G as an F8V star ($T \approx 6250$ K, $\log g \approx 4.3$; Aller et al. 1982), in significant disagreement with the RP04 temperature and gravity. We believe that the GH09 values are based on by far the best data, and for the purpose of this paper, we will adopt their values.

Based on the observations, RP04 asserted that Star G was located at approximately 3 ± 0.5 kpc—consistent with the remnant's distance. They note that this star has solar metallicity, and therefore its kinematic signature was not attributable to being a member of the Galactic halo. They further argued

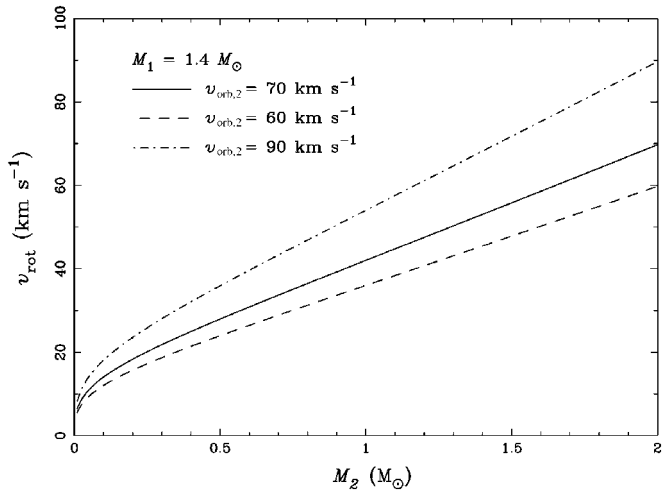

Figure 2. Expected rotation rate for a donor star as a function of its mass at the time of the explosion. The three curves show the results for three final space velocities of the donor star (similar to those suggested by RP04). It is assumed that the white dwarf has a mass of 1.4 $M_\odot$.

that Star G's radial velocity and proper motion were both inconsistent with the distance, a simple Galactic rotation model, and the star being part of the disk population of the Milky Way. The derived physical characteristics of the system were nearly identical to what was proposed by Podsiadlowski (2003) for a typical SN Ia donor star emerging from a single-degenerate system (e.g., U Sco; also see Hachisu et al. 1996; Li & van den Heuvel 1997; Hachisu et al. 1999b; Han & Podsiadlowski 2004; Han 2008). The revision in the stellar parameters by GH09 leads to different distance with a larger uncertainty, but by and large, has not altered the conclusions above. Taken in total, the data provide a rather convincing case for the association of Star G with the Tycho SN.

3. RAPID ROTATION: A KEY SIGNATURE IN SN Ia DONOR STARS

In the single-degenerate SN Ia progenitor channel, mass is transferred at a high rate from a secondary star onto a white dwarf (Nomoto 1982; Nomoto et al. 2007). These high mass transfer rates require that the secondary star overflows its Roche lobe. Due to the strong tidal coupling of a Roche-lobe filling donor, the secondary is expected to be tidally locked to the orbit (i.e., has the same rotation period as the orbital period). At the time of the SN explosion, the donor star is released from its orbit, but will continue with the same space velocity as its former orbital velocity and continue to rotate at its tidally induced rate.

There is a simple relationship between the secondary's rotation velocity ($v_{\rm orb,2}$) and its orbital velocity:

$$v_{\rm rot} = \frac{M_1 + M_2}{M_1}\, f(q)\, v_{\rm orb,2},$$

where $f(q)$ is the ratio of the secondary's Roche-lobe radius to the orbital separation (e.g., given by Eggleton 1983) and $q = M_1/M_2$ is the mass ratio of the components at the time of the explosion. Figure 2 shows the rotational velocity as a function of secondary mass for several values of $v_{\rm orb,2}$ (consistent with RP04s measurement, and at the low end of values expected for a subgiant star), where we assumed that the exploding white dwarf had a mass of 1.4 $M_\odot$.

This estimate is strictly speaking an upper limit, as it does not take into account the angular momentum loss associated with the stripping of envelope material by the SN and any bloating due to the SN heating. The latter would reduce the rotational velocity to first order by a factor equal to the bloating factor (i.e., the ratio of the new to the old radius), but the star would likely find itself in a state where its radius and temperature were atypical of a normal star.

According to the results of Marietta et al. (2000), mass stripping is not likely to be significant if the companion is a main-sequence star or a subgiant. Furthermore, following binary evolution of a main-sequence star, Pakmor et al. (2008) have shown that even less material is stripped. However, if the companion is a giant, it would be stripped of most of its envelope. Such a star would not show any signs of rapid rotation since the initial giant would have been relatively slowly rotating; e.g., if one assumes solid-body rotation in the envelope, the rotation velocity at $\sim$1 $R_\odot$ will only be $\sim$0.5 km s^{-1} for a pre-SN orbital period of 100 d. Moreover, the material at the surface may have expanded from its original radius inside the giant, further reducing the rotational velocity. However, if the stripping is less than estimated by Marietta et al. (2000), then it is possible for the signature of rotation to persist for a giant, albeit at a much lower velocity.

Marietta et al. (2000) also showed that due to the interaction of the SN blast wave with the companion, the secondary may receive a moderate kick of up to a few 10 km s^{-1}, but this kick is generally much lower than $v_{\rm orb,2}$ and therefore does not significantly affect the resulting space velocity.

Finally, we note that the observed rotation velocities are reduced by a factor $\sin i$, where i is the inclination angle. However, because the donor star's rotational axis can be assumed to be parallel to its orbital axis, a minimum observed rotation speed can be computed from the observed peculiar radial velocity (observed radial velocity minus the expected radial velocity of an object at that distance and direction). It is only if the orbital motion (and hence final systemic velocity) is solely in the plane of the sky, that $\sin i$, and therefore, the observed rotation, approaches zero.

4. SUBARU OBSERVATIONS

To investigate the rotational properties of Star G, we were granted time with the Subaru telescope. Our observations of Star G were taken in service mode on the nights of 2005 October 17 and 2005 October 18. Nine spectra were taken with the HDS (Noguchi et al. 1998) with a resolution of $R \simeq 40{,}000$ (measured using the instrumental broadening of the thorium–argon arc lines), an exposure time of 2000 s each (totalling to 5 hr), and a signal-to-noise ratio of about 10 per pixel (measured at 8300 Å with 0.1 Å pixel^{-1}). The HDS features two arms, with each arm feeding a two-chip CCD mosaic. The blue arm covers 6170–7402 Å and the red arm 7594–8818 Å. For the red arm observations, an OG530 filter was used to block contamination from light blueward of our observing window, and data were binned by 4 in both the spatial and spectral directions, resulting in a pixel size of 0.1 Å (at 8000 Å) by 0.″55.

Data were preprocessed using tools provided by the HDS team and then bias-subtracted. We created a mask from bias and flat-fielded frames, where we isolated the echelle orders and flagged bad pixel regions. The data were flat-fielded using internal quartz flats, and the two-dimensional images cleaned of cosmic rays (and checked carefully by eye to ensure there were no unintended consequences) using an algorithm supplied by M. Ashley (2007, private communication). The spectrum

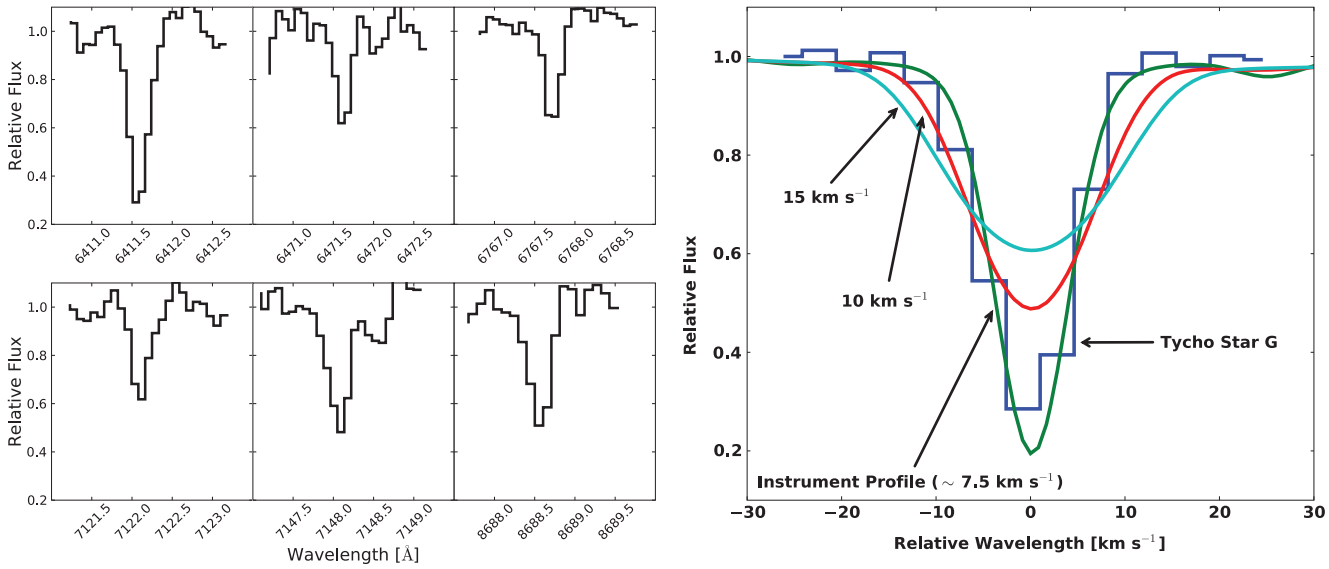

Figure 3. Six observed Fe I line profiles of Star G are shown on the left panel. The right panel shows the combination of these line profiles after normalization to the same equivalent width and compares them to the spectrum of the Sun, which is convolved with three different values for the rotational broadening kernel. Star G does not show significant rotation, indicating $v_{\rm rot} \sin i \lesssim 7.5$ km s^{-1}.

(A color version of this figure is available in the online journal.)

of each echelle order was extracted using IRAF[8] echelle routines, with wavelength calibrations based around low-order fits of a thorium–argon arc. Wavelength calibration of each extracted spectrum was checked against atmospheric O_2, and our solutions were found to be accurate in all cases to within 1 km s^{-1} (Caccin et al. 1985). Unfortunately, we lacked a smooth spectrum standard star for setting the continuum, and we resorted to calculating a median of the spectra (6 Å window) and dividing the spectra through this smoothed median. This unusual method was chosen over the common approach of fitting the spectrum with a polynomial, due to the special characteristics of this observation (low signal-to-noise ratio and a complex instrumental response). While this does not affect the narrow lines our program was targeting, it does affect broad lines such as the Hα and the Ca II IR triplet. The final step was to combine all spectra and remove any remaining cosmic rays (in the one-dimensional spectra) by hand.

5. ANALYSIS AND RESULTS

5.1. Rotational Measurement

To attain the rotational velocity of the candidate star, we measured several unblended and strong (but not saturated) Fe I lines in the spectrum (Wehrse 1974). Since our spectrum only had a combined signal-to-noise ratio of approximately 10, we added the spectra of the lines after normalizing them to the same equivalent width. As a reference we created three synthetic spectra (one broadened only with the instrumental profile, the others with the instrumental profile and $v_{\rm rot} \sin i$ of 10 and 15 km s^{-1}, respectively) with the 2007 version of MOOG (Sneden 1973), using GH09's temperature, gravity, and metallicity. We use a standard value of $\beta = 3/2$ for the limb darkening although the choice of this value is not critical, which we confirmed by checking our results using significantly different values of β. Figure 3 shows the comparison between the synthetic spectra of different rotational velocities and the spectrum of Star G. We have scaled the synthetic spectrum using the equivalent width. This comparison indicates that the stellar broadening (rotational, macroturbulence, etc.) is less than broadening due to the instrumental profile of 7.5 km s^{-1}, and therefore we adopt 7.5 km s^{-1} as our upper limit to the rotation of the star. If one were to adopt RP04's measurements of the peculiar spatial motion, it could be concluded that $\sin i$ is much closer to 1 than 0 (see the end of Section 3 for further explanation) and thus that the rotational speed is $v_{\rm rot} \lesssim 7.5$ km s^{-1}.

5.2. Radial Velocity

To determine the radial velocity, we used 63 lines to measure the shift in wavelength. We find a radial velocity in the topocentric (Mauna Kea) frame of reference of $v_{\rm top} = -92.7 \pm 0.2$ km s^{-1} (the error being the standard deviation of 63 measurements). The conversion from the topocentric to the Galactic LSR for our observations was calculated to be 13.6 km s^{-1} (IRAF task rvcorrect) using the IAU standard of motion. Including the uncertainty in the LSR definition, we find a radial velocity in the LSR for Star G of $v_{\rm LSR} = -79 \pm 2$ km s^{-1}. This is in significant disagreement with that reported by RP04, but agrees with the revised value published by GH09.

5.3. Astrometry

RP04 have measured a significant proper motion for Star G of $\mu_b = -6.1 \pm 1.3$ mas yr^{-1}and $\mu_l = -2.6 \pm 1.3$ mas yr^{-1}. Because Star G is metal rich, and at a distance of $D > 2$ kpc, this measurement provides one of the strongest arguments for Star G being the donor star to Tycho SN. It is almost impossible to account for this proper motion, equivalent to a $v_b = 58\left(\frac{D}{2\ \rm kpc}\right)$ km s^{-1} or three times the disk's velocity dispersion of $\sigma_z = 19$ km s^{-1}, except through some sort of strong binary star interaction.

However, the *Hubble Space Telescope* (*HST*) data present an especially difficult set of issues in obtaining astrometry free of

[8] IRAF is distributed by the National Optical Astronomy Observatories, which is operated by the Association of Universities for Research in Astronomy (AURA) under cooperative agreement with the National Science Foundation.

Table 1
Proper Motions of Stars within 45″ of the Tycho SNR Center

α (hh:mm:ss.ss)	δ (dd:mm:ss.ss)	μ_l (mas yr^{-1})	μ_b (mas yr^{-1})	m_R (mag)	θ (arcsec)	Name
00:25:20.40	+64:08:12.32	−0.90	−0.56	17.05	08.9	c
00:25:18.29	+64:08:16.12	−4.25	−0.81	18.80	10.0	e
00:25:17.10	+64:08:30.99	−1.82	1.78	16.87	20.3	f
00:25:23.58	+64:08:02.02	−1.58	−2.71	17.83	31.1	g
00:25:15.52	+64:08:35.44	1.94	0.83	20.28	31.4	r
00:25:15.08	+64:08:05.95	−0.67	1.49	18.86	33.3	j
00:25:23.89	+64:08:39.33	−0.31	1.08	19.20	33.5	k
00:25:14.74	+64:08:28.16	2.60	1.46	17.45	33.5	n
00:25:14.81	+64:08:34.22	4.05	−2.05	19.35	35.0	q
00:25:13.79	+64:08:34.50	2.32	1.01	19.90	41.3	s
00:25:14.59	+64:07:55.10	−3.94	2.35	19.23	41.7	t
00:25:19.25	+64:07:38.00	1.75	−3.43	16.86	42.1	u
00:25:22.45	+64:07:32.49	81.29	−2.68	19.81	48.7	HP-1

systematic errors. For Star G, these issues include the point-spread function (PSF) on the first epoch WFPC2 image being grossly undersampled, both the Advanced Camera for Surveys (ACS) and WFPC2 focal planes being highly distorted, poor and different charge transfer efficiency across the two *HST* images, and that Star G was, unfortunately, located at the edge of one of the WFPC2 chips, making it especially difficult to understand the errors associated with it. Smaller issues include the small field of overlap between the two images, making the measurement subject to issues of the correlated motions of stars, especially in the μ_l direction.

To cross-check RP04's proper motion of Star G, we have scanned a photographic plate taken in 1970 September on the Palomar 5 m, and compared this to an Isaac Newton 2.5 m Telescope (INT) CCD archive image (INT200408090414934) of the remnant taken in 2004 August. The Palomar plate has an image FWHM of 1.″7, and the INT image 0.″88. While our images have a much larger PSF than the *HST* images, the images have significantly less distortion, are matched over a larger field of view with more stars, have fully sampled PSFs, and were taken across nearly an eight times longer time baseline. The photographic nature of the first epoch does add complications not present in the *HST* data. The nonlinear response of photographic plates causes their astrometry to have systematic effects as a function of brightness (Cannon et al. 2001), especially affecting objects near the plate limit, where single grains are largely responsible for the detection of an object.

The positions of stars on the INT image was matched to the Two Micron All Sky Survey (2MASS) point source catalog (Skrutskie et al. 2006) to get a coordinate transformation (pixel coordinates to celestial coordinates) using a third-order polynomial fit with an rms precision of 40 mas with 180 stars. This fit is limited by precision of the 2MASS catalog and shows no systematic residuals as a function of magnitude, or position. Using this world coordinate system (WCS) transformation, we then derived the positions of all stars on the INT image. The coordinates of 60 uncrowded stars on the Palomar plate were matched to the INT-based catalog, and a third-order polynomial was used to transform the Palomar positions to the INT-based positions. The fit has an rms of 65 mas in the direction of Galactic longitude and 45 mas in the direction of Galactic latitude. We believe the larger scatter in the direction of Galactic longitude is due to the shape of the PSF being slightly nonsymmetric in the direction of tracking on the Palomar plate. This tracking (in right ascension, which is close to the direction of Galactic longitude) causes the position of stars to depend slightly on their brightness. This explanation is supported by a small systematic trend in our astrometric data in μ_l, not seen in μ_b, as a function of m_R. An alternative explanation is that the trend in μ_l is caused by the average motion of stars changing due to Galactic rotation as a function of distance, which is proxied by m_R. We have used the Besançon Galactic model (Robin et al. 2003) to estimate the size of any such effect, and find that the observed effect is an order of magnitude larger than what is expected. The systemic difference between assuming either source of the observed effect is less than 1 mas yr^{-1} in μ_l, and has no effect in our μ_b measurement. In our final proper motions, presented in Table 1, we remove the systematic trend as a function of m_R with a linear function.

To measure the proper motion of each star, we exclude each star from the astrometric transformation fit so as not to bias its proper-motion measurement. Comparing the stellar positions in the 34 yr interval, we find that these 60 stars show an rms dispersion $\sigma_{\mu_l} = 2.1$ mas yr^{-1}and $\sigma_{\mu_b} = 1.6$ mas yr^{-1}. For Star G, we measure $\mu_l = 1.6 \pm 2.1$ mas yr^{-1}and $\mu_b = 2.7 \pm 1.6$ mas yr^{-1} (as seen in Figure 4); this implies that no significant proper motion is detected. We do note that this measurement has a similar precision to that of RP04, is consistent with no observed motion, and is in moderate disagreement with the RP04 measurement.

In Table 1, we present our astrometric measurements of all stars listed by RP04 for which we were able to measure proper motions. We also give the apparent magnitudes in R (partly measured by this work and partly by RP04) and the distance from center θ. Due to crowding caused by the relatively poor resolution of the first epoch photographic plate, several stars are not included that could be measured using *HST*. We include an additional star, not cataloged by RP04, which exhibits high proper motion. This high proper motion star, which was off the WFPC2 images of RP04, we designate HP-1, and has a proper motion of $\mu_l = 81.3$ and $\mu_b = -2.7$ mas yr^{-1}. Due to the distance from the remnant's center, (we estimate HP-1 would have been located 51″ from the remnant's center in 1572), we doubt that this star is connected to the Tycho SN, but we include it for the sake of completeness.

6. DISCUSSION

6.1. A Background Interloper?

A previously unrecognized property for many progenitor scenarios is the rapid postexplosion rotation of the donor (as

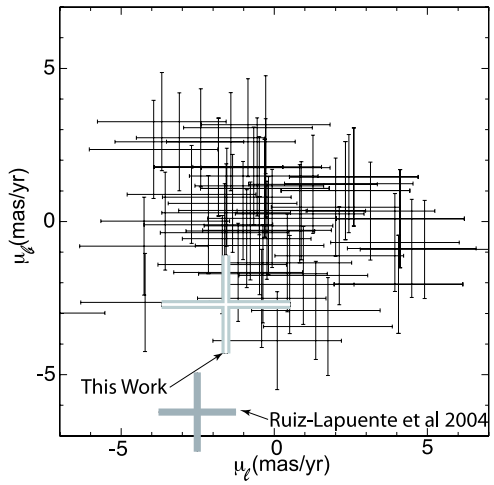

Figure 4. Astrometric motions of 60 stars measured in the Tycho SNR center. The measurements have an rms dispersion of 1.6 mas yr^{-1}. Shown in gray is the proper motion of Star G measured here and by RP04, showing a moderate discrepancy in the two measurements. Our measurement is consistent with no proper motion.

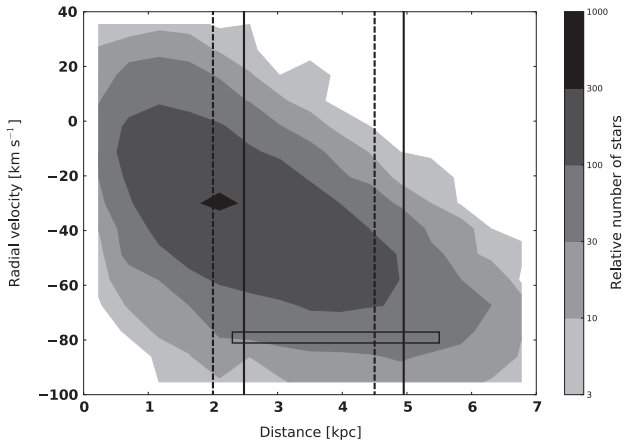

Figure 5. Besançon model for a metal-rich ([Fe/H] > −0.2) Galactic population between 0 and 7 kpc in the direction of Tycho SNR ($l = 120.1$, $b = 1.4$) with a solid angle of 1 deg^2. The remnant's distance is represented by the black dashed lines (as calculated in Section 2). The contours show the radial velocity distribution. Our measured radial velocity corrected to LSR and our distance are shown, with their respective error ranges, as the black rectangle. The distance ranges calculated by GH09 are indicated by the two solid lines. The observed LSR v_r for Star G is mildly unusual for stars at the remnant's distance, and is consistent with the bulk of stars behind the remnant.

described in Section 3). The expected rotation as calculated in Figure 2 is large compared to that expected of stars with a spectral type later than F and should be easily observable. We have shown Star G's rotation to be less ($v_{\rm rot} \sin i \lesssim 7.5$ km s^{-1}) than what is expected of an associated star if the companion was a main-sequence star or subgiant. A red giant scenario where the envelope's bloating has significantly decreased rotation could be consistent with our observation of Star G, and this will be discussed in Section 6.2.

The primary basis for which RP04 selected Star G as a candidate for the donor star to the Tycho SN was the combination of its large peculiar radial velocity and its observed proper motion. In Figure 5, we use the Besançon Galactic model (Robin et al. 2003) to construct an expected set of radial velocities for metal-rich stars in the direction of SN 1572.

Measuring the distance to Star G is a key discriminant in associating the star to the SN explosion. To improve the uncertainty of the distance to the star, due both to temperature and extinction uncertainty, we base our distance on the observed m_K (Skrutskie et al. 2006) and $(V-K)$ color (RP04). We interpolate ATLAS9 models without overshoot (Bessell et al. 1998) to find a theoretical $V-K$ and absolute magnitude for the GH09's values of temperature and gravity. Using a standard extinction law (Cardelli et al. 1989; $A_V = 3.12E(B-V)$ and $A_K/A_V = 0.109$) to match the theoretical and observed colors, we find $A_V = 2.58 \pm 0.08$ mag, $A_K = 0.28 \pm 0.01$ mag, and $E(B-V) = 0.84 \pm 0.05$. To better show the uncertainties, we present our distance moduli scaled to the observed and derived values of extinction, temperature, and gravity. The temperature coefficients were determined by integrating blackbodies of the appropriate temperature with a filter bandpass and fitting a power law to the resulting flux.

$$(m_V - M_V) = 12.93 - 3.12(E(B-V) - 0.84) - 2.5(\log g - 3.85) + 2.5 \log\left(\frac{M}{1\ M_\odot}\right) + 2.5 \log\left(\frac{T_{\rm eff}}{5900}\right)^{4.688}, \quad (1)$$

$$(m_K - M_K) = 12.93 - 0.275(E(B-V) - 0.84) - 2.5(\log g - 3.85) + 2.5 \log\left(\frac{M}{1\ M_\odot}\right) + 2.5 \log\left(\frac{T_{\rm eff}}{5900}\right)^{1.937}. \quad (2)$$

Assuming a companion mass of 1 $M_\odot$, we find $(m - M) = 12.93 \pm 0.75$ mag. This uncertainty is dominated by the precision of $\log g$, and equates to a distance of $D = 3.9 \pm 1.6$ kpc. Star G, within the errors, is at a distance consistent with the remnant. As seen in Figure 5, the observed radial velocity of Star G is consistent with a significant fraction of stars in its allowed distance range. We also note that if Star G is indeed associated with the SN, that it is likely that Star G could have a mass considerably less than 1 $M_\odot$, due to mass transfer and subsequent interaction with the SN, although in this case, the distance to the star would still be consistent with SNR distance.

Ihara et al. (2007) looked for absorption due to Fe I in the remnant's expanding ejecta for 17 stars within the Tycho remnant. No such absorption was seen in the spectrum of Star G, potentially placing it in front of the remnant. However, the amount of Fe I currently within the remnant is uncertain with predicted column densities spanning several orders of magnitude ($0.02 - 8.9 \times 10^{15}$ cm^{-2}; Hamilton & Fesen 1988; Ozaki & Shigeyama 2006). Therefore, we do not believe the lack of significant Fe I 3720 absorption in Star G to be significant.

In summary, we find that Star G's radial velocity, distance, and stellar parameters are all consistent with an unrelated star, but also with it being the donor star. There is disagreement in Star G's measured proper motion. The measurements of RP04 are inconsistent with normal disk stars at the known distance and strongly point to Star G being associated with the SN, whereas the measurements presented here are consistent with a normal disk star, unrelated to the SN. In addition, we have shown that the rotation of Star G is low (confirmed by GH09; $v_{\rm rot} \leqslant 6.6$ km s^{-1}), arguing against association with the SN, as does its off center placement in the remnant. Finally, GH09 have

presented evidence that Star G is strongly enhanced in nickel, an observation that, if confirmed, would strongly point to an association of the star with the SN. If either the high proper motion, or significant nickel enhancement can be confirmed, then it is likely that Star G is the SN donor star. Otherwise, we believe that it is much more likely that Star G is simply an interloper.

6.2. Star G as the Donor Star to the Tycho SN

While the case for Star G's association with the SN is not conclusive, it is intriguing, and we believe it is worthwhile to look for a consistent solution assuming that the association is true. While not a priori probable, a self-consistent model can be constructed in which Star G was the companion, as we shall discuss now.

To make such a model work, Star G has to be a stripped giant that presently mimics a G2IV star. At the time of the explosion, the star would have been a moderately evolved giant (in a binary with an orbital period $\sim$ 100 d). The SN ejecta will strip such a giant of almost all of its envelope (Marietta et al. 2000) due to its low binding energy; only the most tightly bound envelope material outside the core will remain bound. Due to the heating by the SN, even this small amount of material (perhaps a few $\times 0.01\ M_{\odot}$) will expand to giant dimensions, and the immediate-post-SN companion will have the appearance of a luminous red giant. However, because of the low envelope mass, the thermal timescale of the envelope is sufficiently short that it can loose most of its excess thermal energy in 400 yr and now has the appearance of a G2IV star (Podsiadlowski 2003).

A lower mass for Star G (0.3–0.5 $M_{\odot}$) also reduces the distance estimate, and makes the observed radial velocity more unusual for stars at this distance. The expected spatial velocity depends on the pre-SN orbital period and should be in the range of 30–70 km s^{-1} for a period range of 20–200 days (Justham et al. 2009). These velocities are consistent with the inferred spatial velocity of the object relative to the LSR if Star G is at the distance of the remnant, even if no significant proper motion has been measured (see Figure 5).

A stripped-giant companion would link the progenitor to the symbiotic single-degenerate channel (Hachisu et al. 1999a) for which the symbiotic binaries TCrB and RS Oph are well-studied candidates. Indeed, Justham et al. (2009) argued that the ultracool low-mass helium white dwarfs (with masses $\lesssim 0.3\ M_{\odot}$) that have been identified in recent years are most likely the stripped giant companions that survived SN Ia explosions, which could provide some further possible support for such a scenario for Star G.

If the association is real, Star G's displacement to the southeast (SE) of the geometric center of the remnant as defined by radio and X-ray observations might be interpreted as being due to the remnant's interaction with an inhomogeneous ISM. Deep optical images of the remnant do show extended diffuse emission along the eastern and northeastern limbs interpreted as shock precursor emission (Ghavamian et al. 2000). This along with an absence of detected Balmer-dominated optical emission along the whole of the western and southern limbs suggests a density gradient of the local ISM with increasing density toward the northeast (NE). An east–west (E–W) density gradient has also been inferred from detailed radio expansion rate measurements (Reynoso et al. 1997). Such an E–W density gradient could have led to a more rapid expansion toward the west giving rise to a small shift in the apparent geometric center away from the SE without creating a highly distorted remnant. However, there are problems with this explanation. Deviations from spherical symmetry in both radio and X-ray images of the remnant are relatively small (Reynoso et al. 1997; Cassam-Chenaï et al. 2007), and the remnant is most extended along the eastern and northeastern limbs, just where one finds the greatest amount of extended diffuse optical emission. Moreover, the remnant's expansion rate appears lowest toward the NE (P.A. $= 70^{\circ}$), not the SE (Reynoso et al. 1997). Although the argument that Star G's SE displacement from the remnant's current geometric center is a result of an asymmetrical expansion is not strong, it remains a possibility.

The most conclusive way of confirming a stripped-giant scenario for Star G would be an independent, precise measurement of the distance to Star G which in combination with measurements of the gravity and effective temperature would help to constrain Star G's mass. Unfortunately, such a measurement will most likely have to wait for the advent of the *GAIA* satellite. Alternatively, one may be able to single out a stripped giant from a normal G2IV star through nucleosynthesis signatures, specifically evidence for CNO-processed material (or other nucleosynthetic anomalies). While a normal G2IV star is unlikely to show CNO-processed material at the surface, a stripped giant is likely to do so. Unfortunately, the data presented here are not of adequate quality to explore the detailed properties of Star G's atmosphere.

7. OUTLOOK AND FUTURE OBSERVATIONS

Presently, we believe the evidence for Star G's association with the Tycho SN is interesting, but not conclusive. A possible scenario if Star G is the donor star, would be that of a stripped-giant scenario discussed in Section 6. However, there are still other stars that have not been adequately scrutinized. Ihara et al. (2007) have found a star (RP04 Star-E) which may contain blueshifted Fe I lines, indicating their association with the remnant. Unfortunately, the star has neither a significant peculiar radial velocity (Ihara et al. 2007; RP04) nor a significant peculiar proper motion (RP04 and confirmed by our work; see Table 1).

High-resolution spectroscopy of each candidate in the remnant's center is necessary to precisely determine each star's physical parameters. However, the small observed velocities of the remaining stars suggest that the donor star would have needed to be a giant at the time of explosion. Using RP04's observed values, none of the stars in the remnant's center appear consistent with what is expected of a giant star as the donor star except possibly for Star-A. We also note that there is an additional star present in archived *HST* images, not cataloged in RP04, offset from RP04's Star-A by 0.″5E and 0.″2N at $m_V = 16.8$, $(B - V) = 1.0$. This star, near the remnant's center, has a color consistent with an F star (assuming that it is behind the bulk of the line of sight reddening), but it will require adaptive optics to obtain its spectrum given its proximity to the 13th magnitude Star A. This star could potentially be a nongiant progenitor.

If future observations are unable to pinpoint a viable donor star, other progenitor scenarios will have to be considered. These include the double-degenerate scenario, or a scenario where there is a long time delay between the accretion phase of a donor star onto the white dwarf, and the ultimate SN explosion.

We thank the Subaru HDS team for taking these observations in service mode. This paper makes use of data obtained from the Isaac Newton Group Archive which is maintained as part of the CASU Astronomical Data Centre at the Institute of

Astronomy, Cambridge. This publication makes use of data products from the Two Micron All Sky Survey, which is a joint project of the University of Massachusetts and the Infrared Processing and Analysis Center/California Institute of Technology, funded by the National Aeronautics and Space Administration and the National Science Foundation. This work also makes use of POSS I data. The National Geographic Society-Palomar Observatory Sky Atlas (POSS I) was made by the California Institute of Technology with grants from the National Geographic Society. This work makes use of VLA data operated by the National Radio Astronomy Observatory. The National Radio Astronomy Observatory is a facility of the National Science Foundation operated under cooperative agreement by Associated Universities, Inc. W.E.K., B.P.S., and M.A. are supported by the Australian Research Council (grant DP0559024, FF0561481). This paper was conceived as part of the Tokyo Think Tank collaboration, and was supported in part by the National Science Foundation under grant PHY05-51164. This work was supported in part by World Premier International Research Center Initiative (WPI Program), MEXT, Japan, and by the Grant-in-Aid for Scientific Research of the Japan Society for the Promotion of Science (18104003, 18540231, 20540226) and MEXT (19047004, 20040004). Additionally, we thank Pilar Ruiz Lapuente and her team for the valuable discussions we had in regards to the manuscript. We also thank our referee, who provided us with a very detailed and thorough analysis of the first manuscript and subsequent revisions.

REFERENCES

Aller, L. H., et al. 1982, Landolt-Börnstein: Numerical Data and Functional Relationships in Science and Technology (Berlin: Springer)
Altavilla, G., et al. 2004, MNRAS, 349, 1344
Bessell, M. S., Castelli, F., & Plez, B. 1998, A&A, 333, 231
Caccin, B., Cavallini, F., Ceppatelli, G., Righini, A., & Sambuco, A. M. 1985, A&A, 149, 357
Canal, R., Méndez, J., & Ruiz-Lapuente, P. 2001, ApJ, 550, L53
Cannon, R., Hambly, N., & Zacharias, N. 2001, in ASP Conf. Ser. 232, The New Era of Wide Field Astronomy, ed. R. Clowes, A. Adamson, & G. Bromage (San Francisco, CA: ASP), 311
Cardelli, J. A., Clayton, G. C., & Mathis, J. S. 1989, ApJ, 345, 245
Cassam-Chenaï, G., Hughes, J. P., Ballet, J., & Decourchelle, A. 2007, ApJ, 665, 315
Eggleton, P. P. 1983, ApJ, 268, 368
Ghavamian, P., Raymond, J., Hartigan, P., & Blair, W. P. 2000, ApJ, 535, 266
Gooch, R. 1996, in ASP Conf. Ser. 101, Astronomical Data Analysis Software and Systems V, ed. G. H. Jacoby & J. Barnes (San Francisco, CA: ASP), 80
Hachisu, I., Kato, M., & Nomoto, K. 1996, ApJ, 470, L97
Hachisu, I., Kato, M., & Nomoto, K. 1999a, ApJ, 522, 487
Hachisu, I., Kato, M., Nomoto, K., & Umeda, H. 1999b, ApJ, 519, 314
Hamilton, A. J. S., & Fesen, R. A. 1988, ApJ, 327, 178
Han, Z. 2008, ApJ, 677, L109
Han, Z., & Podsiadlowski, P. 2004, MNRAS, 350, 1301
Hernandez, J. I. G., Ruiz-Lapuente, P., Filippenko, A. V., Foley, R. J., Gal-Yam, A., & Simon, J. D. 2009, ApJ, 691, 1 (GH09)
Iben, I. J. 1997, in NATO ASIC Proc. 486: Thermonuclear Supernovae, ed. P. Ruiz-Lapuente, R. Canal, & J. Isern (Dordrecht: Kluwer), 111
Ihara, Y., Ozaki, J., Doi, M., Shigeyama, T., Kashikawa, N., Komiyama, K., & Hattori, T. 2007, PASJ, 59, 811
Justham, S., Wolf, C., Podsiadlowski, P., & Han, Z. 2009, A&A, 493, 1081
Krause, O., Tanaka, M., Usuda, T., Hattori, T., Goto, M., Birkmann, S., & Nomoto, K. 2008, Nature, 456, 617
Leonard, D. C. 2007, ApJ, 670, 1275
Li, X.-D., & van den Heuvel, E. P. J. 1997, A&A, 322, L9
Marietta, E., Burrows, A., & Fryxell, B. 2000, ApJS, 128, 615
Noguchi, K., Ando, H., Izumiura, H., Kawanomoto, S., Tanaka, W., & Aoki, W. 1998, Proc. SPIE, 3355, 354
Nomoto, K. 1982, ApJ, 253, 798
Nomoto, K., Saio, H., Kato, M., & Hachisu, I. 2007, ApJ, 663, 1269
Ozaki, J., & Shigeyama, T. 2006, ApJ, 644, 954
Pakmor, R., Röpke, F. K., Weiss, A., & Hillebrandt, W. 2008, A&A, 489, 943, 0807.3331
Patat, F., et al. 2007, Science, 317, 924
Podsiadlowski, P. 2003, arXiv:astro-ph/0303660
Reynoso, E. M., Moffett, D. A., Goss, W. M., Dubner, G. M., Dickel, J. R., Reynolds, S. P., & Giacani, E. B. 1997, ApJ, 491, 816
Robin, A. C., Reylé, C., Derrière, S., & Picaud, S. 2003, A&A, 409, 523
Ruiz-Lapuente, P. 2004, ApJ, 612, 357
Ruiz-Lapuente, P., et al. 2004, Nature, 431, 1069 (RP04)
Skrutskie, M. F., et al. 2006, AJ, 131, 1163
Sneden, C. 1973, ApJ, 184, 839
Wehrse, R. 1974, A List of All Fraunhofer Lines of the Rowland Tables Arranged by Elements (Heidelberg: Universität)
Winkler, P. F., Gupta, G., & Long, K. S. 2003, ApJ, 585, 324